Egyptian Journal of Chemistry

Designing and Producing pH Sensitive Warning Clothes with different Fabric Constructions using Chromic Materials

Amina L. Mohamed [a*], **Ghalia E. Ibrahim** [b], **Eman R. Mahmoud** [b], **and Fatma A. Abd El-Hamied** [b]

[a] *National Research Centre (Scopus affiliation ID 60014618), Textile Research and Technology Institute, Pretreatment, Finishing of Cellulose-based Fibre Department, 33 El-Behouth St. (former El-Tahrir str.), Dokki, P.O. 12622, Giza, Egypt*

[b] *Helwan University, Faculty of Applied Arts, Spinning and Weaving Department, Giza, Egypt*

Abstract

The subject of pH-sensitive textiles has advanced significantly in recent decades. Chrome textiles may be utilized in a variety of applications as flexible sensors. In this study, garments were created utilizing color-changing materials that are sensitive to pH shift and various fibers (cellulose and synthetic fibers), as well as diverse combinations, to shield laboratory personnel from the risks of acid and alkaline gases. All of the samples used in the study were made from cotton, viscose, and polyester. By combining different wefts, numbers, and fabric compositions, designers were able to create functional fabrics that may act as sensors, alerting wearers to danger and sudden color changes. Different methods have been used to build halo-chromium-based textile pH sensors that are responsive to the pH and alkalinity of various fabrics. The study's findings demonstrate that halo chromic sensors may be made utilizing the pH-indicating Cresol Red dye. Additionally, the Sol-gel method was used to encapsulate the Cresol Red pH Indicator in a silica net, producing clear and uniform tablets from chitosan doped with isopropyl acrylamide, a surfactant. The spectra demonstrated that the encapsulated CR was effective at sensing pH and alkalinity since it kept its structure in terms of its reaction to pH under neutral circumstances. With the change in pH, this therapy changed hue. The tissue density affects how these sensors respond. It is taken into account that this treatment's halo chrome behavior differs from that of the dye in the solution. In the end, several staining methods have succeeded in creating pH probes for treated tissues.

Introduction

Smart fabrics have been the focus of several investigations during the past ten years. [1] The vision of this type of textile is to create textile products exhibiting dynamic functionalities by combining these textiles with smart materials or integrated computing power so fabrics can sense and react to various environmental conditions and stimuli. Smart textiles are used in several fashion products, furnishing, and technical textiles applications. [2-4]

An emerging trend in the field of smart textiles is the use of color-changing materials, often known as chameleon textiles or (chromic textiles), which may change color in response to a variety of external stimuli. [1, 5]

Thermochromism (induced by temperature), photochromism (induced by light), halochromism (induced by pH), [6] electrochromism (induced by electricity), solvatochromism (induced by the polarity of solvent), etc. are different types of chromism (chromic material) depending on the nature of the stimulus. [1]

Dyes, which are materials that change color in a reversible way as a result of external stimuli, are a crucial component of smart materials [7]. Additionally, the coloring compounds known as halo chromes are susceptible to pH variations.

The fact that these materials can be applied to textiles in a variety of straightforward and flexible ways, where the color change is instantly apparent to everyone and may thus be utilized as a first, on-destructive warning signal, makes them incredibly important in warning fabrics. [5]

_____

According to this, the number of studies devoted to chromic materials has dramatically increased in recent years due to the development of wearable sensors. [8] For instance, incorporating sensing capabilities into textiles can have a positive impact on a variety of industries, including sports performance, military applications, lab coats, and the healthcare sector. [9] In addition to these uses, had a significant impact in the sectors of the environment, industry, food, biology, and medicine. [10] As a result, wearable textiles can track the physical condition of a soldier or athlete as well as the environment. They may also track the pH of a wound dressing to track the progress of a wound's healing without removing the gauze, for example. [6, 11, 12]

The PH-value is an important parameter in many situations, and photochromic textiles can be used for a variety of applications. For example, in this research, it was incorporated in protective clothing, specifically in lab coats, to indicate the presence of alkali or acid vapors in the lab working environment, protecting the user from the dangers of these vapors.

So, the resultant cloth may effectively be treated with pH indicators. The weft and warp were made of cotton and polyester fibers, respectively. Its distinctive functional qualities of durability, high flexibility, and high resistance to abrasion by friction, acid and alkali resistance, and softness of viscose, as well as its widespread use in the production of products that need high absorption and high durability, make it suitable for a variety of applications. Polyester and viscose fabrics are used in the weft of the fabrics produced.

The usual hopsack 2/2 fabric structure was also employed in the study. As opposed to other textile structures, the typical hopsack 2/2 fabric structure is distinguished by an abundance of interlocks per square unit, giving the fabric excellent durability. This is the result of the variance in the number of interlocks per square unit of each textile structure. Numerous methods have been used to obtain pH-sensitive textile fabrics. These substances are known as halo-chromic materials and are pH-sensitive. [7]

One of the most often used PH indicators and a member of the most significant group of pH-sensitive dyes is Cresol Red. With Cresol red shifting color from yellow to orange at pH levels below 3.6 and from yellow to red at pH levels above 7.5, it serves as an effective pH indicator. An encapsulation was created for cresol Red dye to preserve the color longer in alkaline solutions. [7].Due to the ever-growing number of applications, porous silica nanoparticles are drawing a lot of attention to the creation of porous materials. This is mostly because of its special qualities. [13].

Mesoporous materials offer important properties such as resistance to heat, sunlight, moisture, chemicals, and aging. They also have high specific surfaces, large pores, and distinctive pores. [14] Additionally, it was utilized in the textile sector. With the use of silicone technology, the textile industry may create specialized textiles and apparel that completely satisfies the practical requirements of contemporary living. The development of practical fabrics and high-performance textiles is made possible by silicone technology, which benefits customers who are stylish, cozy, or cost-conscious. [15, 16]

The construction of pH sensors may be accomplished using the sol-gel method, which is also regarded as an indication package. Due to its uses in chemical and environmental areas, pH is a significant photochemical sensor. [17]

In this study, different fabric construction has been treated using pH-sensitive dye, then the treated fabrics were taken and exposed to fumes of acids and bases, recording the color difference and also recording its ability to return to normal by recording the difference in wavelength using a UV/Vis device at 440, and 550 nm, and collecting that curves, which demonstrated the effectiveness of this method.

2. Experimental
2.1 Materials

Tetraethyl orthosilicate (TEOS), cetyltrimethylammonium bromide (CTAB), and triethanolamine (TEA) all were analytical grade and purchased from Sigma -Aldrich. N-isopropyl acrylamide monomer (NIPAM) and chitosan (CS) polymer were used from across organics and were used to produce a pH-responsive copolymer. Ammonium persulfate (APS) was provided by Merck and was used as an initiator. Cresol red dye is used as a pH indicator and chloroform was purchased from Merck. All chemicals are used directly without purification

2.2. Methods
2.2.1. Manufacture of fabrics

In this research, 9 woven samples were woven in the Textile Design and Technology produced using a Dobby loom. All samples in the research were produced with cotton warp yarns of 50/2 Ne and a warp set of 36 ends/cm. Three materials of weft yarns were used cotton, viscose, and polyester, with three different yarns count (30/1, 30/1, and 150 deniers). Three weft sets were also used 30, 35, and 40 picks/cm with fabric construction regular hopsack 2/2. The specification of produced fabrics is illustrated in Table 1

_____

Table 1: specifications of the produced fabrics

Fabric construction	Warp type	Warp set	Weft type	Weft sets	Code
Regular hopsack 2/2	Cotton	36 ends/cm	Cotton	30	I
				35	II
				40	III
			Polyester	30	IV
				35	V
				40	VI
			Viscose	30	VII
				35	VIII
				40	IX

2.2.2. Synthesis of Mesoporous silica nanoparticles

According to Mohamed et. al. [18], long-chain quaternary ammonium surfactants were used to create mesoporous silica nanoparticles (MSN). 50 mL round bottom, a three-necked flask filled with 20 mL of deionized water. After that, 1 mmol each of CTAB and TEA were dissolved in water and gently stirred at 65°C for 1 hour. The previous CTAB-TEA mixture was carefully added, and 1mmol of TEOS was carefully added, dispersed in 4 mL of chloroform, and swirled continuously for a further 24 hours using a magnetic stirrer (350 rpm). MSNs were collected by 12,000 rpm centrifugation. To get rid of the remaining reactants, ethanol, and deionized water were used to wash the nanoparticles. The nanoparticles were extracted with a 0.6 weight percent NH_4NO_3 in ethanol solution at 60°C for 12 hours, then washed three times with anhydrous ethanol to get rid of the CTAB and TEA. Produced nanoparticles were lyophilized to have dry nanoparticle powder.

2.2.3. Encapsulation of dye into synthesized mesoporous silica

Cresol red dye was encapsulated onto the porous surface of MSNs using a solvent evaporation process to create MSN-encapsulated cresol red nanoparticles. In a nutshell, MSNs (10 mg) and cresol red solution (10 mL, 1 mg/mL) were combined and stirred at 400 rpm for 12 hours. Cresol red dye nanoparticles that were MSN-encapsulated were then gathered by centrifugation.

2.2.4. Preparation of pH-responsive poly (N-isopropyl acrylamide-grafted chitosan) (PNIPAM-g-CS) copolymer

The (PNIPAM-g-CS) copolymer was synthesized by using the free radical addition polymerization process. In a nutshell, 2 percent acetic acid was dissolved in 1 g of medium molecular weight chitosan, which was then agitated for 3 hours in a nitrogen environment. Drop by drop, 4 g of NIPAM was added to the CS solution after being dissolved in 30 ml of distilled water. After increasing the

temperature of the reaction to 60°C, 0.08 g of the APS initiator (dissolved in 10 ml of distilled water) was added to the reaction mixture drop by drop. Under a nitrogen environment, the process was running for three hours.

2.2.5. Preparation of pH-responsive fabric

Cresol red nanoparticles with MSN encapsulation were applied to the textile fabric using the pad dry cure process, either on their own or in combination with CS-g-PNIPAM graft copolymer. A solution containing 2 g/l of nonionic surfactant was used to wash the fabric for 40 minutes at 80°C before application, and the fabric was then dried at room temperature. The fabric was then immersed in a first bath solution that contained sodium hypophosphite 5 g/L and butane tetracarboxylic acid (BTCA) 10 g/L at 160°C for two minutes then dried at 90°C for five minutes. The fabric was immersed for 15 minutes in the second bath with a 5 percent concentration of the polymer/dye encapsulated MSN combination, then the fabrics were squeezed, dried at 90°C, and cured at 160°C for 5 minutes.

2.3. Characterizations

Several tests were carried out to evaluate the performance of samples under study, these were:-
1. Fabric weight, this test was carried out according to the ASTM Standard Test Method (D3776/D3776M − 09a (Reapproved 2017)). [19]
2. Fabric thickness, this test was carried out according to the ASTM Standard Test Method (D1777 - 96) (Reapproved 2002). [20]
3. The abrasion resistance, of this test was measured according to ASTM Standard Test Method (ASTM D 4966 - 98) [21]
4. Roughness, this test was measured according to ASTM Standard Test Method (D7127 - 13) using a Surf coder (1700a) [22]
5. pH sensitivity evaluation
    1. Sensor Ph.: This test was performed by Data Color 600 User's Guide Part No. 4230-0395M Rev 1, January 2007; it is a kind of color evaluation measuring and identification instrument. Standard (LAV, SAV, USAV, Barium-coated MAV)

To test the fabrics, an aqueous ammonium hydroxide solution (35 %, 5 ml) or hydrochloric acid (37 %, 5 ml) was placed in a 10 mL test tube. The fabric sample (was placed near the top of the test tube to generate ammonia gas or hydrochloric gas at room temperature and atmospheric pressure demonstrating immediate color change due to exposure (see scheme 1). The photographs of the treated fabric before and after sensing ammonia vapors (at a different time)

evolved using data color from 350 – 800 nm and expressed as absorbance. The reversibility was monitored by observing λ max at the UV/Vis absorption maxima at 440 and 526 nm at ambient temperature. The absorption spectra were recorded for each cycle.

On a carry-UV/VIS spectrophotometer, the UV/VIS spectra of free cresol red (CR), encapsulated CR, and encapsulated CR in the presence of CTAB surfactants in acid and basic solutions were obtained.

3-Results and discussion
3.1. Characterization of chitosan-co-PNIPAAM microgel

In the free radical addition polymerization reaction system, chitosan and poly-NiPAAm may interact in a variety of ways, including electrostatic and hydrogen interactions (between chitosan hydroxyl groups and poly-NiPAAm amide functions), as well as covalent bonding as a result of radical formation. The crucial stage in the copolymerization reaction's process is the radical degradation of chitosan. However, it has been demonstrated that in free radical initiated copolymerization, the main hydroxyl groups of chitosan played a role in the generation of microradicals, which may interact with electrophilic functional groups to generate covalent bonds. Additionally, the C6-OH reactive group of chitosan was connected with the chemical structure of the grafting copolymers poly-NiPAAm. In summary, primary hydroxyl functional groups (C6-OH reactive groups) can be used to produce the covalent connection between chitosan and poly-NiPAAm. Additionally, it has been suggested that anionic persulfate (from the initiator) may get immobilised inside broken chitosan chains due to electrostatic attraction. **[23]**

As a result, chitosan play dual functions in the reaction system. On the one hand, they operate as surfactants, which accelerate polymerization, while on the other, the degraded chitosan chain inhibits free radicals, which slows down polymerization.

The FT-IR spectra of chitosan-co-PNIPAAM are shown in **Figure 1**. After the microgel was formed, the strong and sharp peak at 3350 cm^{-1} that was attributed to the hydroxyl and amino groups of chitosan transformed into a strong and wide peak about 3440 cm^{-1}. Due to the interaction via hydrogen bonding, the absorption bands at 1460 and 1651 cm^{-1} are attributed to the overlapping vibration bands of the stretching vibration of carboxylate groups from chiyosan (1590 and 1416 cm^{-1}) with the amide I bands from PNIPAAm (1640 cm^{-1}). The existence of PNIPAAm is further demonstrated by the sharp band at 1533 cm^{-1} (s, amide II, N-H) in the NIPAAm spectrum, which grows wider with lower intensity in the spectra of the hydrogels at around 1548 cm^{-1} (m).
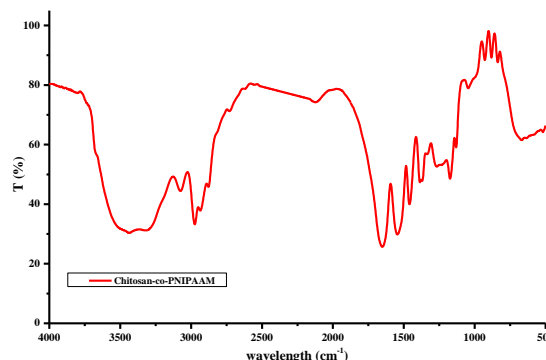

Figure 1: FT-IR, Particle size of chitosan-co-PNIPAAm microgel

3.2. Preparation and characterization of silica nanoparticle

The sol-gel-produced mesoporous silica particles in the current study had an average diameter of 124, 162 nm, perfect and uniform spherical morphologies, and a very smooth outer surface (see Figure 2)

In the sol-gel method, the head groups of CTAB are combined after the silica precursors have been hydrolyzed. The contact between the surfactant and silica precursor might be either an electrostatic force or a hydrogen bond, depending on the kind of surfactant.

The reaction solution's pH and ammonia concentration has an impact on the size of the nano-silica particles as well. Particle size grows as ammonia concentration rises or when the pH is high (see Figure 2). simply that beyond pH 7, condensed species become ionized and repulsive to one another. Due to silica's higher solubility above pH 7, particles grow through particle aggregation and decrease in quantity when highly soluble microscopic particles dissolve and reprecipitate on longer, less soluble particles. This procedure is known as Ostwald ripening. [24, 25]

UV/Vis spectra

The three colors of cresol red (CR)—acid form (orange), neutral form (yellow), and base form (red)—respectively correspond to the absorption peak bands around 420 nm, 525 nm, and roughly 580 nm (Scheme 1). The π-π* and n-π* transitions are responsible for these peaks. Before being exposed to the pH effect, the free CR's absorption spectra differ somewhat from that of the encapsulated CR in silica (Figure 3).

For the free CR in solution, only one absorption band at 435 nm was seen (Figure 3), but two absorption bands at 449 and 525 nm were seen for the encapsulated CR in silica. When the CR is enclosed in silica, the 435 nm peak undergoes a

redshift of around 14 nm (Figure 3). This phenomenon is explained by the silanol groups' partial protonation of cresol red (Scheme 2).

This implies that there are two forms (the acidic and neutral forms). The existence of modest Vander Walls forces between the molecules of the surfactant and the CR species that have been protonated by the silanol group is most likely what is causing this phenomenon. In contrast to the encapsulated CR spectra, the spectrum of the CR embedded in silica in the presence of CTAB revealed one high-intensity absorption band at 445 nm. This is most likely due to CTAB molecules acting as a delaying agent for the protonation of CR by the silanol network, which only produces the neutral form of CR (Figure 3, Scheme 2).
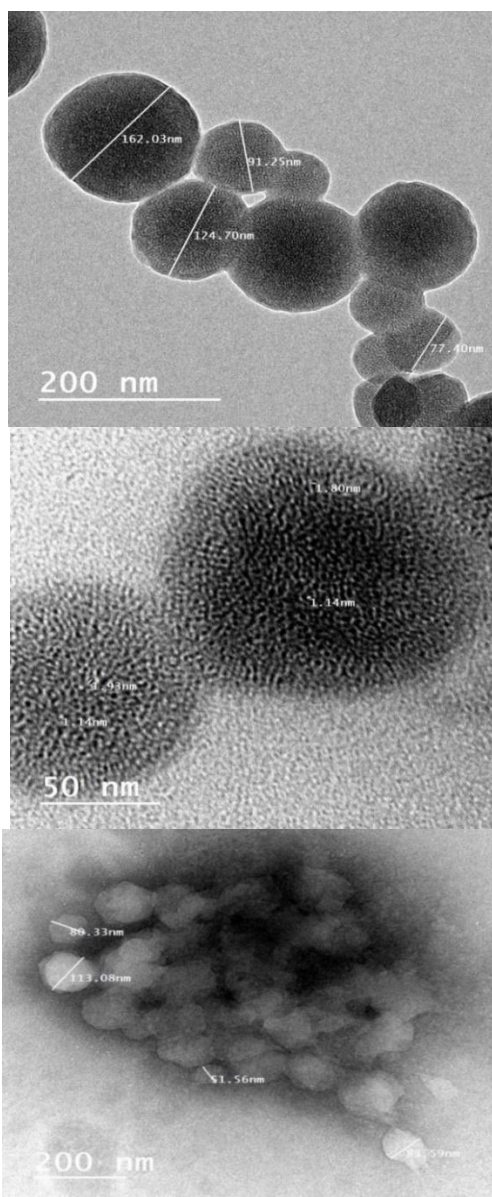

Figure 2: TEM micrograph of the silica nanoparticles

(a) Silica only, (b) silica and dye, and c) Silica and gel.

Scheme 1: color change of Cresol red upon changing pH (acidic, neutral, and basic)
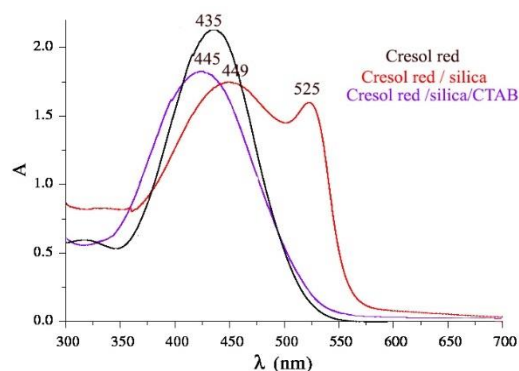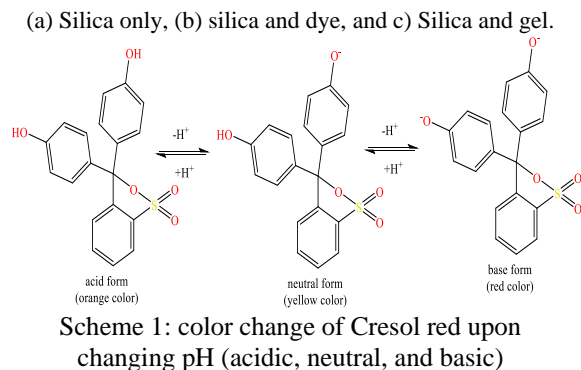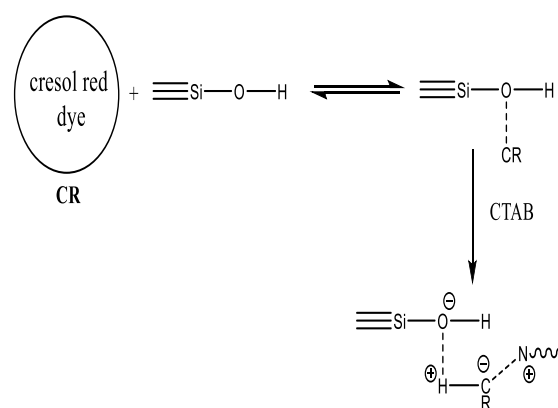

Figure 3: Absorption spectra a cresol red, cresol red /silica, and cresol red /silica/CTAB

Scheme 2: Sol-gel encapsulation of CR in the presence of CTAB

3.3. Characterization of treated fabrics
3.3.1. Morphological behavior

The morphological behavior of the fabric's surface structure before and after treatment, as well as the morphological behavior of treated textiles. Images demonstrate that the surfaces of textiles made from cotton, polyester, and viscose before treatment are smooth and soft, but these surfaces become rough after treatment (see Figure 4). This demonstrates that the silica-infused gel treatment, which coated every surface of the textile structure, gave the fabrics a textured surface.
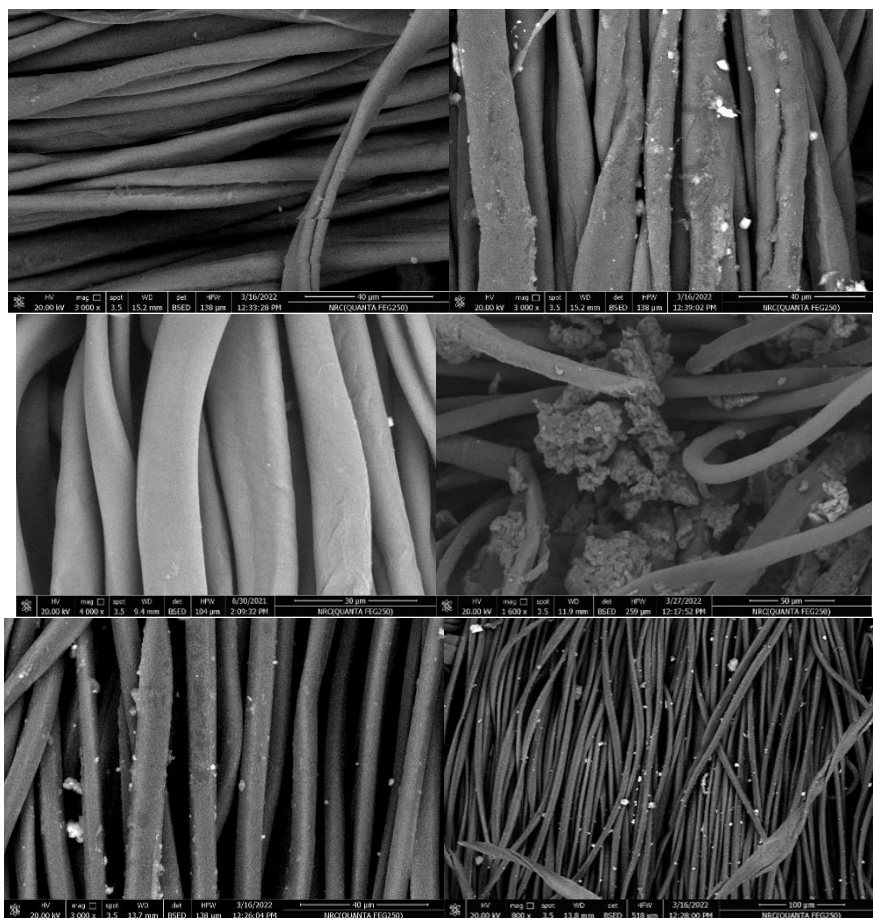
_____

Figure 4: FE-SEM micrograph of the treated fabrics with prepared materials (pH-responsive poly (N-isopropyl acrylamide-grafted chitosan) (PNIPAM-g-CS) copolymer)
a) cotton blank fabric, b) cotton treated fabric, c) polyester blank fabric, d) polyester treated fabric, E) viscose blank fabric, f) viscose treated fabric

3.3.2. pH sensitivity test

When the encapsulated CR/CTAB was exposed to ammonium hydroxide solution 0(NH4OH; 35 percent) or hydrochloric acid, there were three or two forms present (HCl; 37 percent). The ultimate form is always basic (in the case of NH4OH) or acidic (in the case of HCl), but the starting form varies depending on the situation (almost neutral). In the case of encapsulated CR/CTAB, three forms are present, and the interaction with sodium hydroxide or hydrochloric acid solution caused the color to shift from orange (acid form) to yellow (neutral form) and eventually to red (basic form).

The behavior of the encapsulated CR/CTAB is consistent with the idea that in this system, the CR was in the protonated or partially protonated form, so the color changed from yellow to orange and finally to red. encapsulated CR/CTAB provides change between the acid form (orange color)

In addition, for treated fabrics after exposing to the basic acidic vapor, the absorption has recorded the changing in the color over a certain time from 1 to 5 min

For all treated fabrics, it is clear from Figure 5 to Figure 7 that the weft number set in all investigated fabrics has affected the sensitivity of fabric against pH. It found that the weft set number 35 provides the best sensitivity compared to 30 and 40.

For cotton fabrics, it is clear from Figure 5 that for basic medium, weft set 30 provides the highest intensity which decreased upon increasing the weft set number and both 35 and 40 provide almost the same intensity. The peaks didn't decrease even after 5 min and it is still at the same intensity. On the other hand, for acidic medium, weft set 35 provides the highest intensity which decreased upon increasing in the weft set number and both 30 and 40 provide almost the same intensity. The peaks were decreased as the time increased over 5 min which provide the reversibility of the color to the normal stage.

_____

Figure 5: effect of both acidic and alkaline pH on the treated cotton fabric on the color changing
I: Weft sets 30, II: Weft sets 35, and III: Weft sets 40

Figure 6: effect of both acidic and alkaline pH on the treated polyester fabrics on the color changing
IV: Weft sets 30, V: Weft sets 35, and VI: Weft sets 40

Figure 7: effect of both acidic and alkaline pH on the treated viscose fabrics on the color changing
VII: Weft sets 30, VIII: Weft sets 35, and IX: Weft sets 40

For polyester fabrics, it is clear from Figure 6 that for basic medium, weft set 35 provides the highest intensity which decreased upon increasing the weft set number and both 30 and 40 provide almost the same intensity. At the 35 weft set, the peaks didn't decrease even after 5 min and it is still at the same intensity but at other weft sets 30 and 40, the peaks decreased as the time increased over 5 min which provide the reversibility of the color to normal stage. On the other hand, for acidic medium, weft set 30 provides the highest intensity which decreased upon increasing in the weft set number and both 35 and 40 provide almost the same intensity. The peaks were decreased as the time increased over 5 min which provide the reversibility of the color to the normal stage.
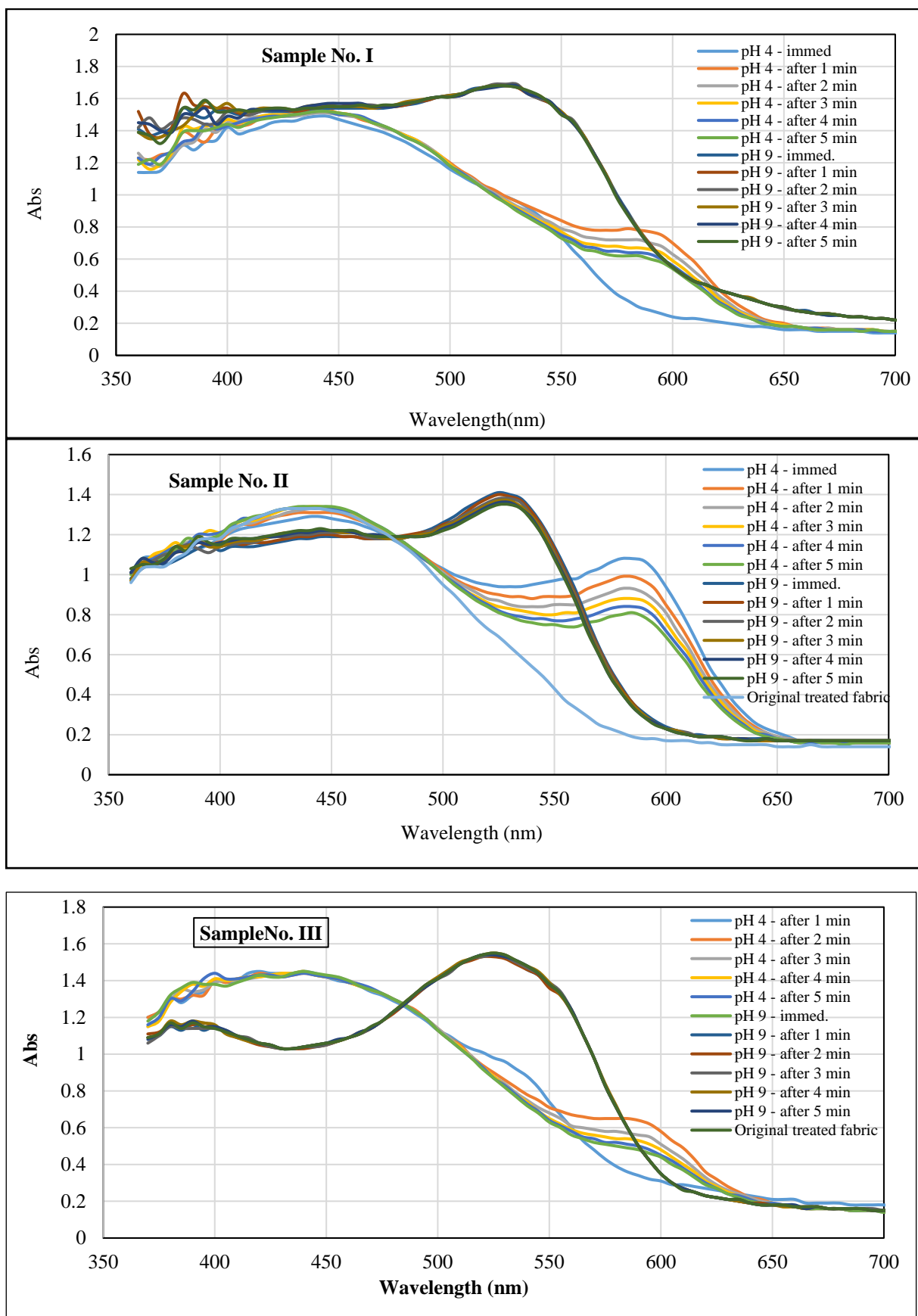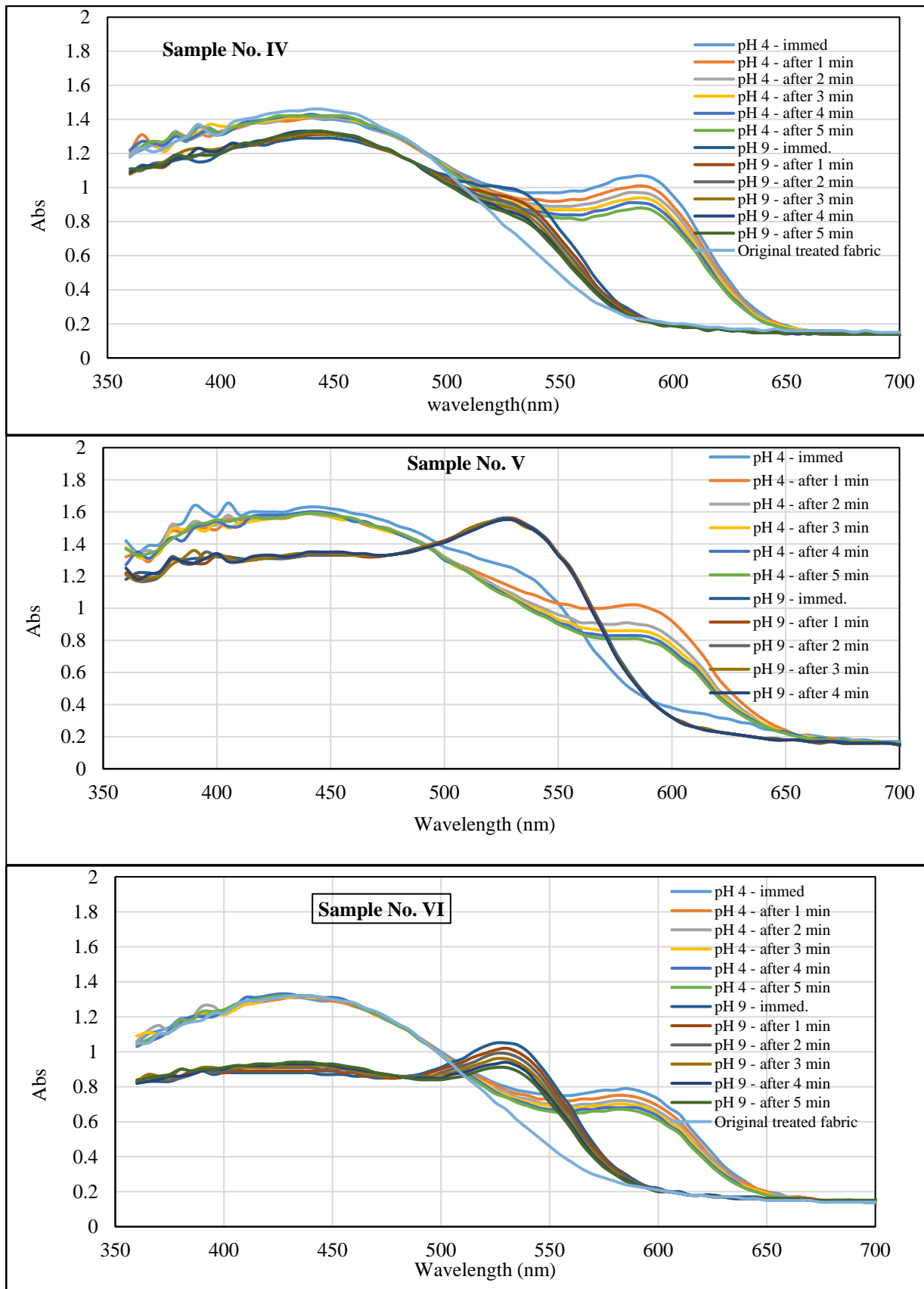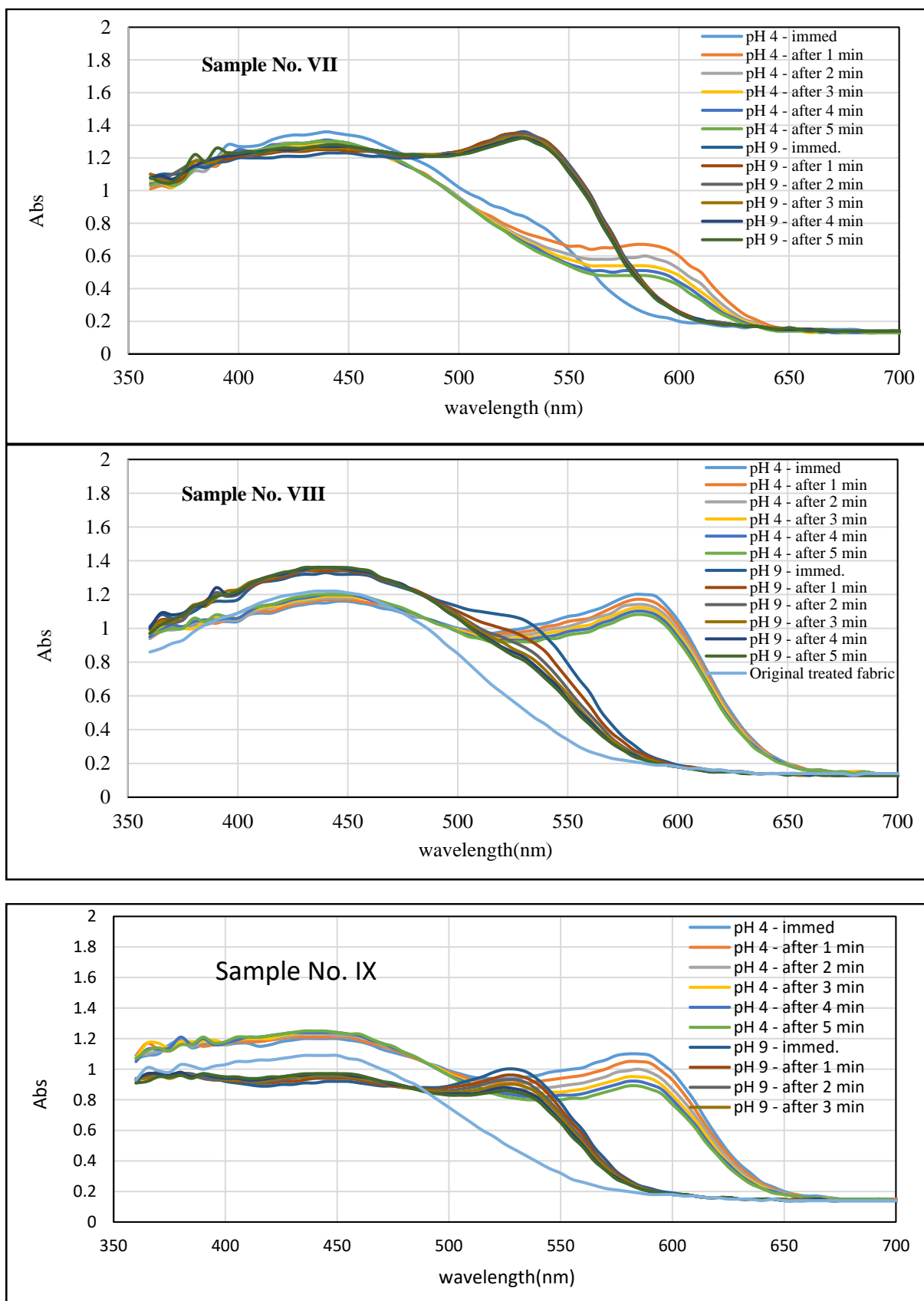
For viscose fabrics, it is clear from Figure 7 that for basic medium, weft set 30 provides the highest intensity which decreased upon increasing the weft set number and both 35 and 40 provide almost the same intensity. At 30 wefts set, the peaks didn't decrease even after 5 min and it is still at the same intensity or showing a slightly decreased but at other

weft sets 35 and 40, the peaks decreased as the time increased over 5 min which provides the reversibility of the color to normal stage. On the other hand, for acidic medium, weft set 35 and 40 provide the highest intensity which decreased upon increasing in the weft set number and 30 wefts set provide lower intensity. The peaks at all wefts set were decreased as the time increased over 5 min which provide the reversibility of the color to the normal stage.

3.3.3. Effect of treatment on fabric properties
3.3.3.1. Effect of treatment on tensile strength and elongation at a break

Results of tensile strength and elongation at a break on samples under study are presented in Figure 8 and Figure 9. Results were statistically analyzed for the data Listed.

It is clear from Table 2 that the polyester fabric records the highest tensile strength and elongation at break values, followed by viscose and then cotton before and after treatment.

	Cotton	Polyester 30	Viscose	Cotton	Polyester 35	Viscose	Cotton	Polyester 40	Viscose
before treatment	121	125	123	123	129	126	125	131	128
After treatment	110.11	120	115.62	113.16	123.84	119.7	116.25	127.07	122.88

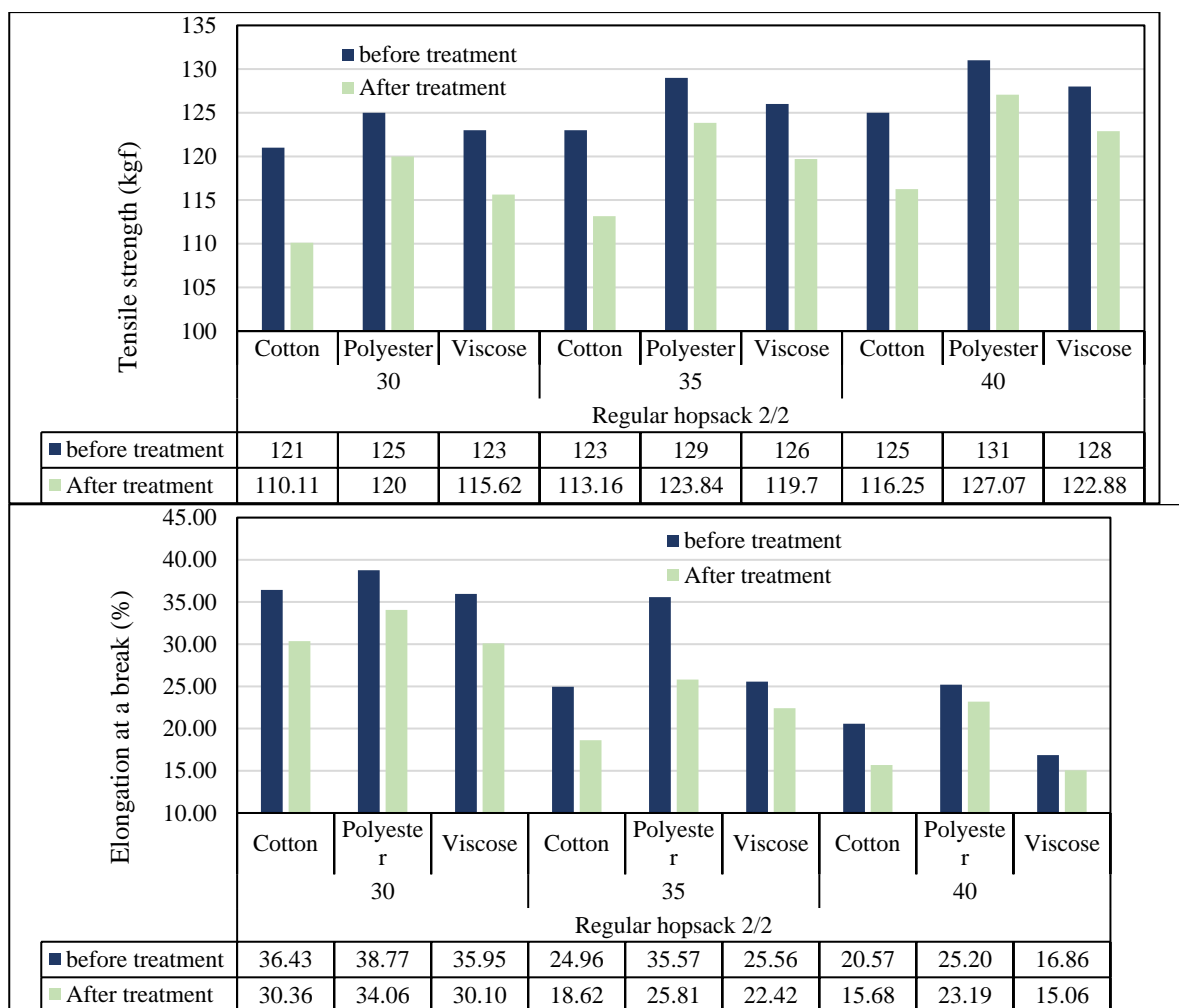|	Cotton	Polyester 30	Viscose	Cotton	Polyester 35	Viscose	Cotton	Polyester 40	Viscose
before treatment	36.43	38.77	35.95	24.96	35.57	25.56	20.57	25.20	16.86
After treatment	30.36	34.06	30.10	18.62	25.81	22.42	15.68	23.19	15.06

Figure 8: Effect of fabric type at different wefts set on the tensile strength and elongation at a break before and after treatment

It is clear from Figure 8 and Figure 9 that there is a strong correlation between the difference in the weft set of fabrics yarn and the tensile strength and elongation at a break, as the density of the weft threads per centimeter increases, the tensile strength was decreased and elongation at a break of fabrics increases when all textile specifications are constant. This is due to the increase in the number of weft sets compared to warp sets. As a result, the percentage of impregnation inside the fabrics increases, and thus frictions between yarns increase, which in the end leads to an increase in the tensile strength and elongation at a break.

In addition, upon treatment tensile strength and elongation at a break for all fabrics are decreased as the treatment could attack the crosslinked bonds between the chain, and it was observed that the decrease in the tensile strength and increase in the elongation at a break for 40, 35, and 30 wefts set respectively.

Furthermore, from Table 2, the correlation coefficient for tensile strength is equal or closer to 1 with all fabrics and followed the following order:

cotton > viscose > polyester fabric, and the correlation coefficient for elongation at a break is closer to 1 with all fabric and followed the following order: viscose > cotton > polyester fabric which provides best effect upon treatment on all investigated wefts set.

3.3.3.2. Effect of Treatment on Fabric Weight

The results of experiments on samples under study are presented in Figure 10. Results were statistically analyzed for the data Listed.

It is clear from Table 3 that the viscose fabric record the highest weight values, followed by cotton and then polyester Because of its high ability to absorb moisture and material from the treatment bath, and that's because of the low degree of polymerization, short chains, and an increase in the percentage of amorphous places in the filaments, which allows a greater degree of absorption of the treatment materials and thus increase the weight.
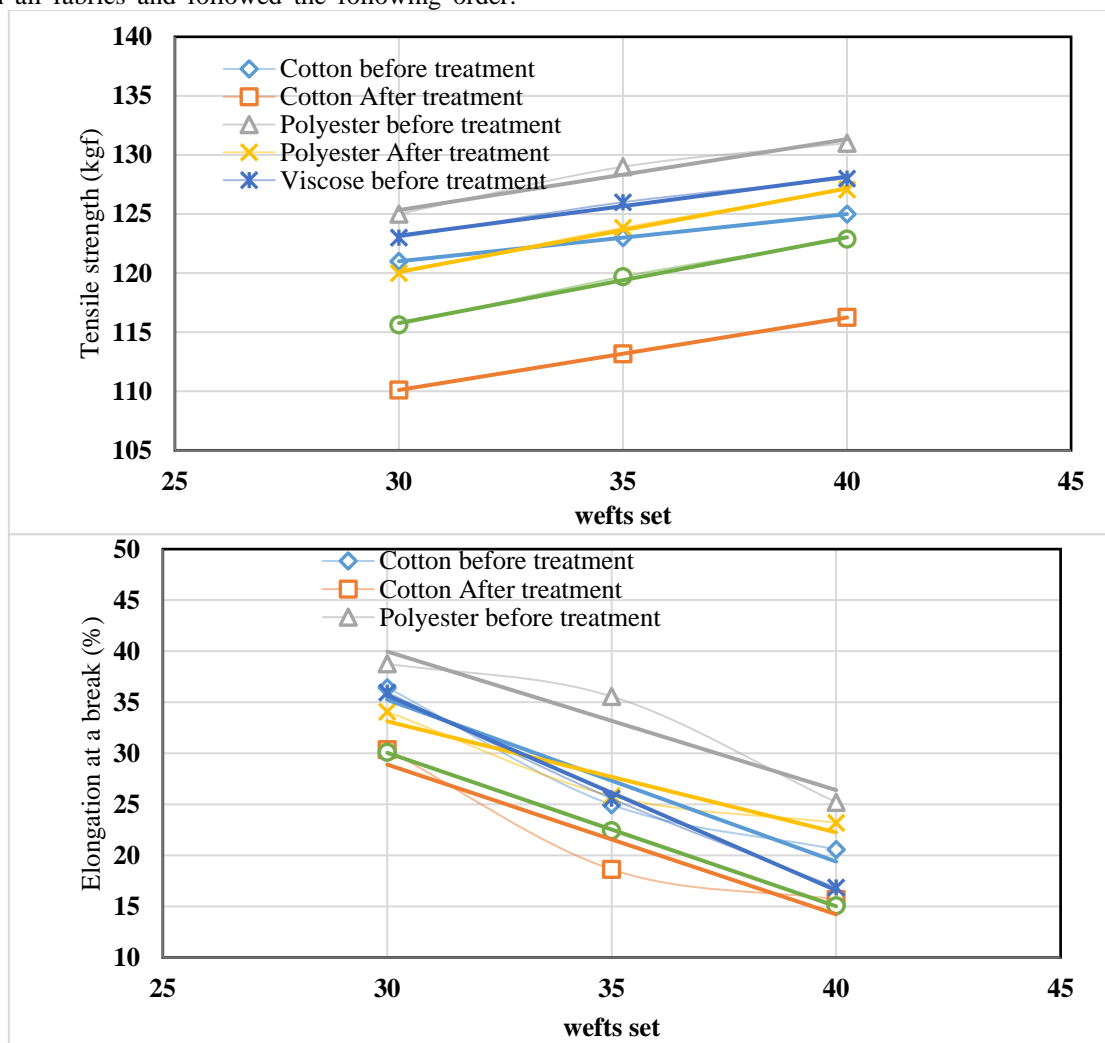

Figure 9: Effect of fabric type at different wefts set on regression equation and correlation coefficient of the tensile strength and elongation at a break before and after treatment

_____

Table 2: regression equation and correlation coefficient of the tensile strength and elongation at a break before and after treatment

		Tensile strength (kg/f)		Elongation at a break (%)	
		Regression equation	Correlation coefficient	Regression equation	Correlation coefficient
Cotton	Before treatment	y = 0.4x + 109	R² = 1	y = -1.5856x + 82.814	R² = 0.9375
	After treatment	y = 0.614x + 91.683	R² = 1	y = -1.4677x + 72.925	R² = 0.8931
Polyester	Before treatment	y = 0.6x + 107.33	R² = 0.9643	y = -1.3572x + 80.68	R² = 0.9149
	After treatment	y = 0.707x + 98.892	R² = 0.9975	y = -1.0876x + 65.752	R² = 0.918
Viscose	Before treatment	y = 0.5x + 108.17	R² = 0.9868	y = -1.9097x + 92.965	R² = 0.9974
	After treatment	y = 0.726x + 93.99	R² = 0.9949	y = -1.5033x + 75.144	R² = 0.9999

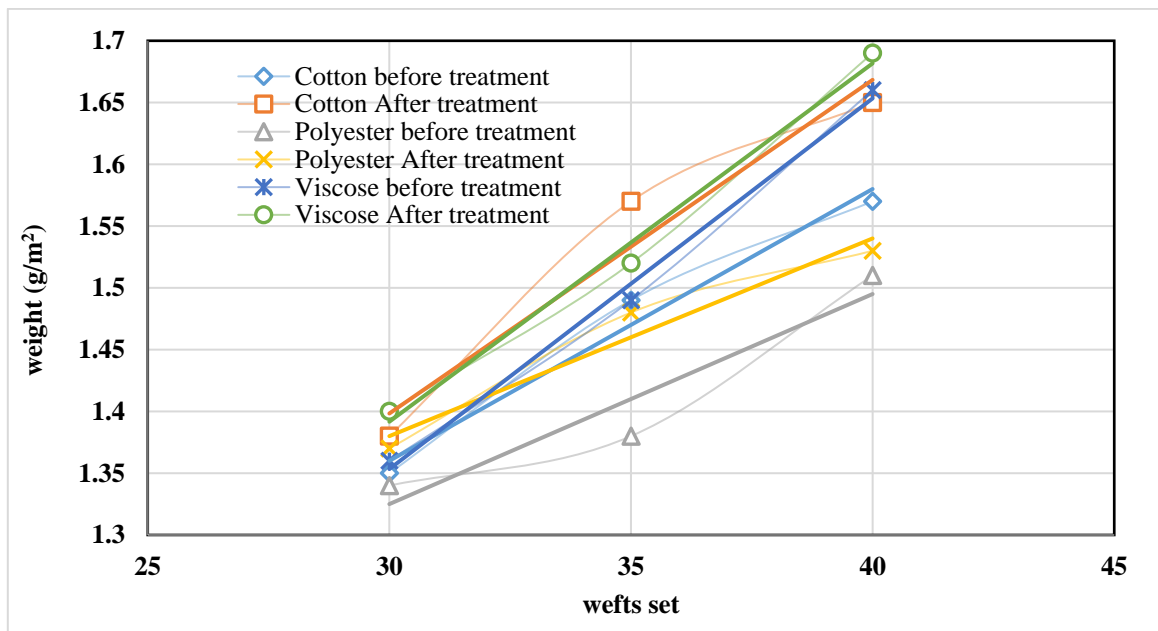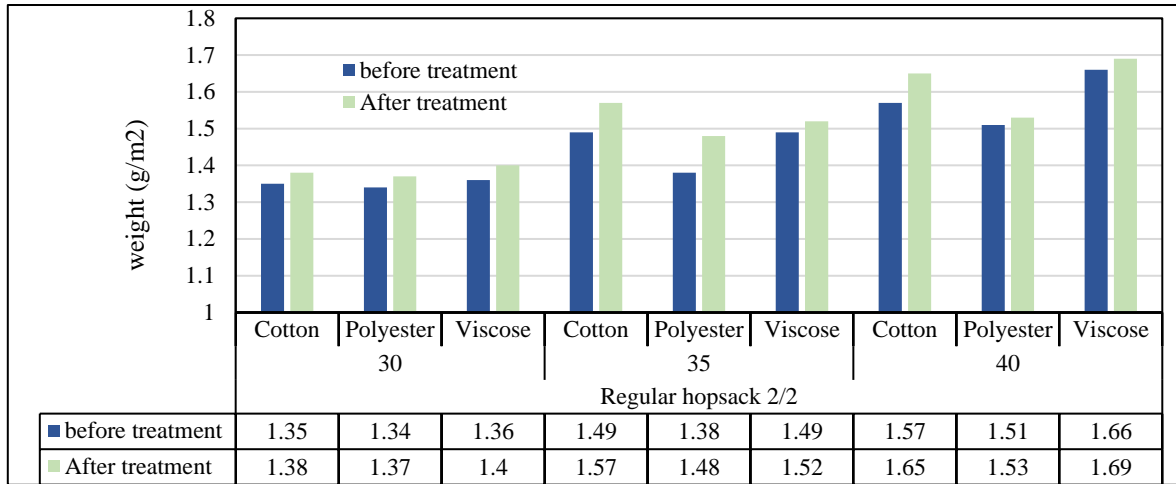|	Cotton	Polyester	Viscose	Cotton	Polyester	Viscose	Cotton	Polyester	Viscose
		30			35			40	
before treatment	1.35	1.34	1.36	1.49	1.38	1.49	1.57	1.51	1.66
After treatment	1.38	1.37	1.4	1.57	1.48	1.52	1.65	1.53	1.69

Figure 10: Effect of fabric type at different wefts set on the weight before and after treatment

Table 3: regression equation and correlation coefficient of the weight before and after treatment

		Regression equation	Correlation coefficient
Cotton	Before treatment	y = 0.022x + 0.7	R² = 0.9758
	After treatment	y = 0.027x + 0.5883	R² = 0.9476
Polyester	Before treatment	y = 0.017x + 0.815	R² = 0.9146
	After treatment	y = 0.016x + 0.9	R² = 0.9552
Viscose	Before treatment	y = 0.03x + 0.4533	R² = 0.9941
	After treatment	y = 0.029x + 0.5217	R² = 0.9902

_____

It is clear from Figure 10 that there is a strong correlation between the difference in the wefts set of polyester yarn and the weight, as the density of the weft threads per centimeter increases, the weight per square meter of fabrics increases when all textile specifications are constant. This is due to the increase in the number of wefts (several wefts) in cm increases. As a result, the percentage of impregnation inside the fabrics increases, and thus the length of the thread increases, which in the end leads to an increase in weight.

In addition, upon treatment, all fabric weights are increased as the treatment makes a thin film on the surface of the fabric, and it observed that the increase in weight is about 22, 20, and 18 % for 30, 35, and 40 wefts set respectively.

Furthermore, from Table 3. The correlation coefficient is closer to 1 with viscose fabric which provides the best effect upon treatment on all investigated wefts set.

3.3.3.2. Effect of treatment on fabrics Thickness

It is clear from Figure 11 that the cotton fabric records the highest thickness rates, followed by viscose and then polyester when regular hopsack 2/2 structure for investigated wefts set.

It is clear from Figure 11 that there is a direct relationship between the difference in the number of picks/cm of cotton fabric and the thickness, where the higher the number of picks/cm, the greater the thickness as shown in the figure. This is because the number of wefts / unit increases with the increase in the number of wefts /cm increases the percentage of impregnation stored inside the fabrics, and thus increases its thickness, and the differences are not significant.

In addition, upon treatment, all fabric thickness is increased as the treatment makes a thin film on the surface of the fabric. it observed that the polyester fabric provides the lowest increase in thickness followed by viscose and then cotton which confirms the highest increase in thickness for the 30, 35, and 40 wefts set respectively.

Furthermore, from Table 4, the correlation coefficient is closer to 1 after treatment with polyester fabric followed by viscose and then cotton fabric which provides the best effect upon treatment on all investigated wefts set and provides a more homogeneous and stable treatment.
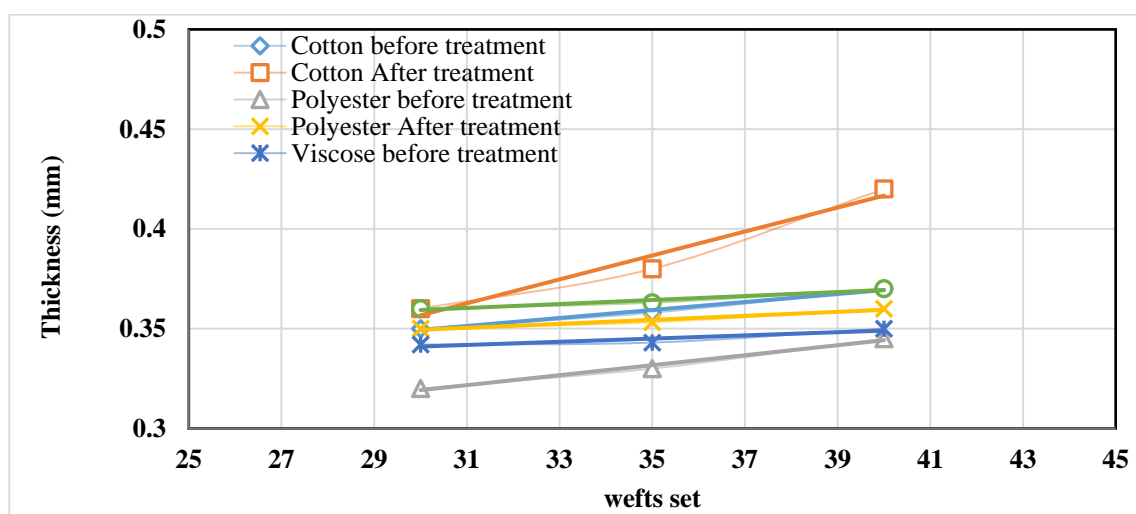

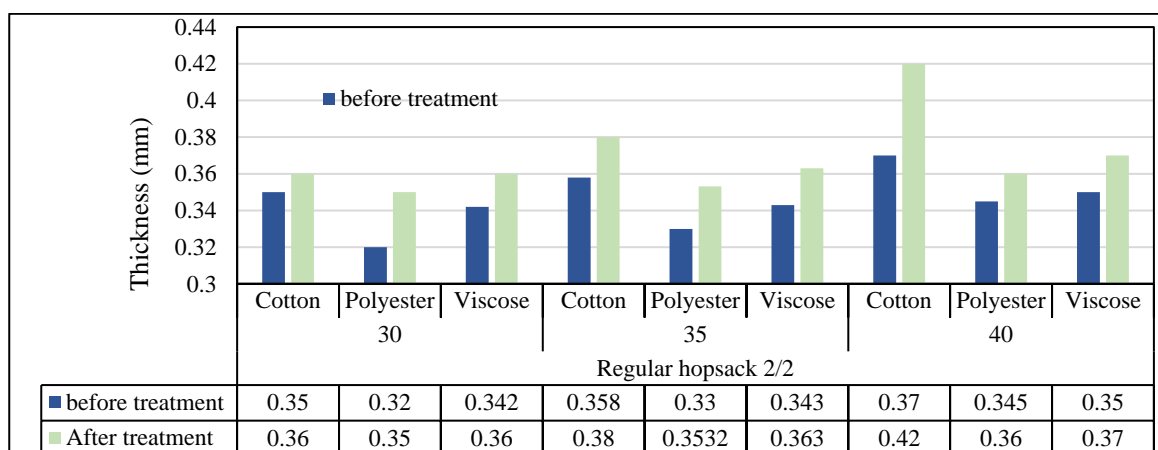|	Cotton	Polyester	Viscose	Cotton	Polyester	Viscose	Cotton	Polyester	Viscose
		30			35			40	
				Regular hopsack 2/2					
before treatment	0.35	0.32	0.342	0.358	0.33	0.343	0.37	0.345	0.35
After treatment	0.36	0.35	0.36	0.38	0.3532	0.363	0.42	0.36	0.37

Figure 11: Effect of fabric type at different wefts set on the thickness before and after treatment

_____

Table 4: regression equation and correlation coefficient of the thickness before and after treatment

		Regression equation	Correlation coefficient
Cotton	Before treatment	y = 0.002x + 0.2893	R² = 0.9868
	After treatment	y = 0.006x + 0.1767	R² = 0.871
Polyester	Before treatment	y = 0.0025x + 0.2442	R² = 0.9868
	After treatment	y = 0.001x + 0.3194	R² = 0.9586
Viscose	Before treatment	y = 0.0008x + 0.317	R² = 0.8421
	After treatment	y = 0.001x + 0.3293	R² = 0.9494

3.3.3.3. Effect of Treatment on fabric Abrasion resistance

It is clear from Figure 12 that polyester fabric has the highest friction values, followed by cotton, then viscose before and after treatment. This is due to the durability of the polyester material, which increases the rate of Abrasion resistance due to its strength, as the strength of polyester filaments is 6.3-9.5 grams/denier.

It is clear from Figure 12 that there is a strong direct relationship between the wefts set 40 and 35 of the polyester material, in contrast to 30, where the higher picks/cm, the greater the friction due to the high cohesion of the threads.

In addition, upon treatment, all fabric friction cycle is increased by about 5 cycles for cotton and viscose fabric and show increasing about 15 cycles for polyester fabric as the treatment make a thin film on the surface of the fabric. this confirms that the friction cycle was increased upon increasing in the wefts set.

Furthermore, from Table 5, the correlation coefficient is equal or very close to 1 before and after treatment with all fabrics which provides the best effect upon treatment on all investigated wefts set and provides a more homogeneous and stable treatment.
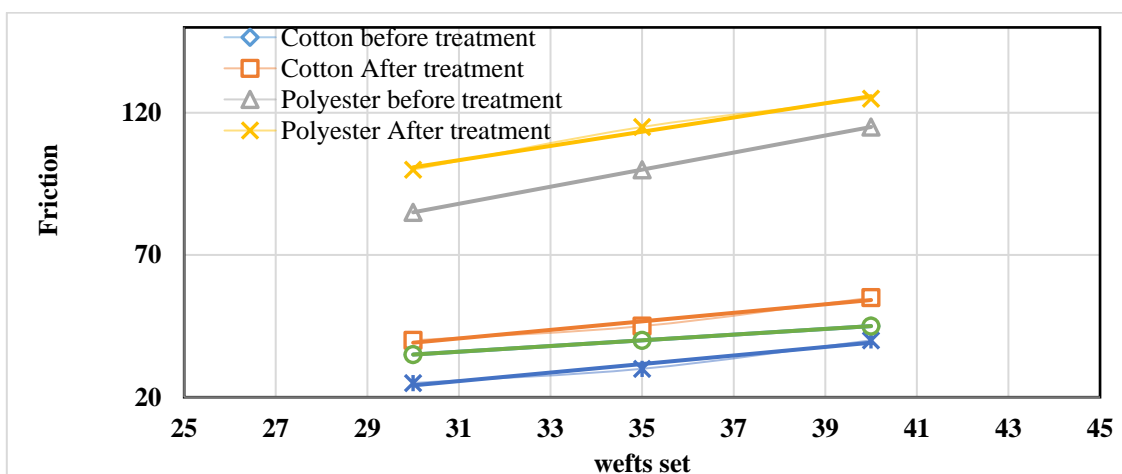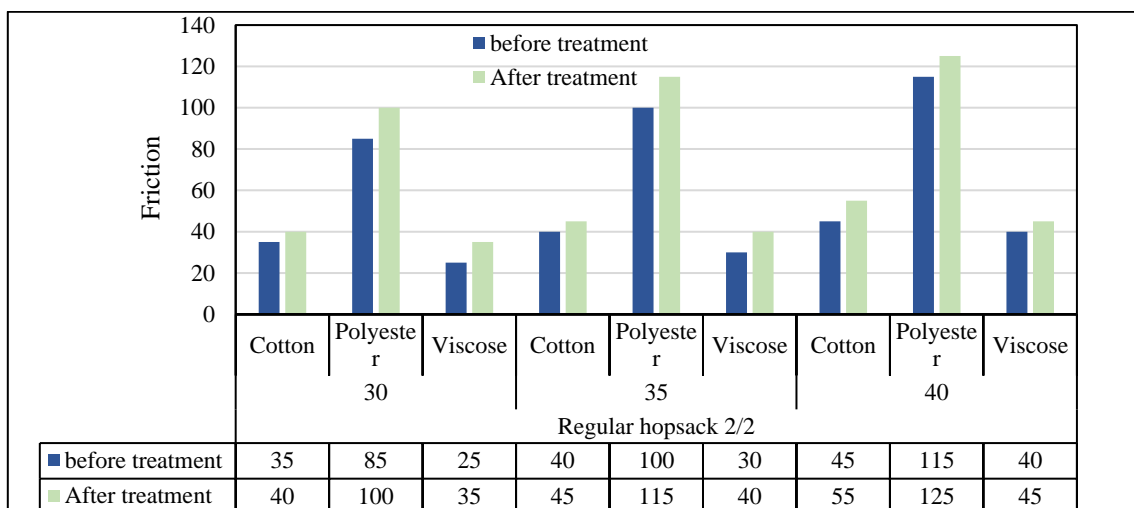

	Cotton	Polyester	Viscose	Cotton	Polyester	Viscose	Cotton	Polyester	Viscose
		30			35			40	
before treatment	35	85	25	40	100	30	45	115	40
After treatment	40	100	35	45	115	40	55	125	45

Regular hopsack 2/2

Figure 12: Effect of fabric type at different wefts set on the friction before and after treatment

_____

Table 5: regression equation and correlation coefficient of the friction before and after treatment

		Regression equation	Correlation coefficient
Cotton	Before treatment	y = x + 5	R² = 1
	After treatment	y = 1.5x - 5.8333	R² = 0.9643
Polyester	Before treatment	y = 3x - 5	R² = 1
	After treatment	y = 2.5x + 25.833	R² = 0.9868
Viscose	Before treatment	y = 1.5x - 20.833	R² = 0.9643
	After treatment	y = x + 5	R² = 1

3.3.3.4. Effect of Treatment on Roughness

It is clear from the Figure 13 that all investigated fabrics with 40 picks/cm achieved the highest roughness rate, followed by 35 picks/cm and then 30 according to the following order cotton > viscose > polyester before and after treatment.

It is clear from Figure 13 that there is a strong direct relationship between the wefts set and roughness, the lower in the roughness is due to the high cohesion of the threads.

In addition, upon treatment, all fabric roughness is increased for all investigated fabrics and shows an increase in the surface roughness as the treatment makes a thin film on the surface of the fabric. this confirms that the roughness was increased upon increasing in the wefts set.

Furthermore, from Table 6, the correlation coefficient is equal or very close to 1 before and after treatment with cotton fabric followed by viscose fabric and then polyester fabric which provide the best effect upon treatment on all investigated wefts set, and provide a more homogeneous and stable treatment.
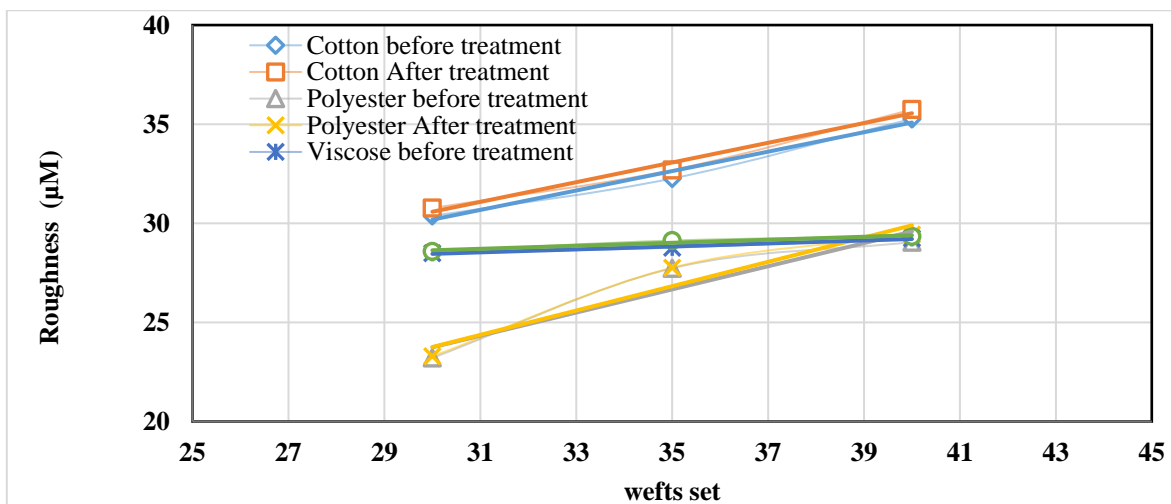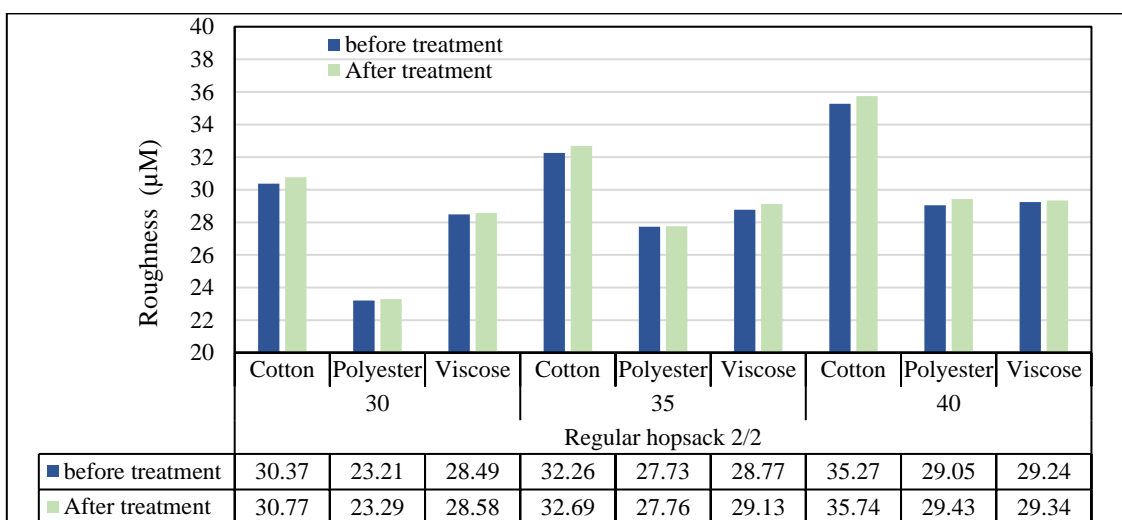

	Cotton	Polyester	Viscose	Cotton	Polyester	Viscose	Cotton	Polyester	Viscose
		30			35			40	
before treatment	30.37	23.21	28.49	32.26	27.73	28.77	35.27	29.05	29.24
After treatment	30.77	23.29	28.58	32.69	27.76	29.13	35.74	29.43	29.34

Regular hopsack 2/2

Figure 13: Effect of fabric type at different wefts set on the roughness before and after treatment

_____

Table 6: regression equation and correlation coefficient of the roughness before and after treatment

		Regression equation	**Correlation coefficient**
Cotton	Before treatment	y = 0.49x + 15.483	R² = 0.9829
	After treatment	y = 0.497x + 15.672	R² = 0.9831
Polyester	Before treatment	y = 0.584x + 6.2233	R² = 0.909
	After treatment	y = 0.614x + 5.3367	R² = 0.9352
Viscose	Before treatment	y = 0.075x + 26.208	R² = 0.9791
	After treatment	y = 0.076x + 26.357	R² = 0.9375

4. Conclusion

This study shows that pH-sensitive textile materials can be obtained with different fabric structures and they provide excellent sensitivity to changes in the color upon changing the pH. Furthermore, this treatment didn't affect the mechanical properties after treatment.

The methods (sol-gel) show great potential and showed that it is an effective technique for obtaining a pH sensor, as transparent homogeneous discs of trapped CR were prepared. In the presence of cetyltrimethylammonium bromide (CTAB). The CTAB, which have a major role in the pH range of action.

Acknowledgments

Author Declarations

The authors declare that the data supporting the findings of this study are available in the article

The authors declare that there is no conflict of interest.

References

[1]. L. Van der Schueren, K. De Clerck, The use of ph-indicator dyes for ph-sensitive textile materials, Textile Research Journal 80(7) (2010) 590-603.

[2]. M. Mohamed, M. Abd El-AAty, S. Moawaed, A. Hashad, E. Abdel-Aziz, H. Othman, A.G. Hassabo, Smart textiles via photochromic and thermochromic colorant, J. Text. Color. Polym. Sci. 19(2) (2022) 235-243.

[3]. A.G. Hassabo, M. Zayed, M. Bakr, H.A. Othman, Chromic dyes for smart textile: A review, Letters in Applied NanoBioScience 12(4) (2023) LIANBS124.161.

[4]. J. Chakravarty, T.A. Edwards, Intelligent (or hi-tech) textiles for monitoring health conditions, Medical textiles from natural resources, Elsevier2022, pp. 373-393.

[5]. M. Kert, J. Skoko, Formation of ph-responsive cotton by the adsorption of methyl orange dye, Polymers 15(7) (2023) 1783.

[6]. L. Leite, V. Pais, C. Silva, I. Boticas, J. Bessa, F. Cunha, C. Relvas, N. Ferreira, R. Fangueiro, Halochromic textiles for real-time sensing of hazardous chemicals and personal protection, Materials 16(8) (2023) 2938.

[7]. T.-T. Li, S. Li, F. Sun, B.-C. Shiu, H.-T. Ren, C.-W. Lou, J.-H. Lin, Ph-responsive nonwoven fabric with reversibly wettability for controllable oil-water separation and heavy metal removal, Environ. Res. 215 (2022) 114355.

[8]. P. Bamfield, M. Hutchings, Chromic phenomena: Technological applications of colour chemistry, Royal Society of Chemistry2018.

[9]. A.G. Hassabo, N. Gamal, A. Sediek, F. Saad, B.M. Hegazy, H. Elmorsy, H. Othman, Smart wearable fabric using electronic textiles – a review, J. Text. Color. Polym. Sci. 20(1) (2023) 29-39.

[10]. D. Staneva, R. Betcheva, J.-M. Chovelon, Optical sensor for aliphatic amines based on the simultaneous colorimetric and fluorescence responses of smart textile, J. Appl. Polym. Sci. 106(3) (2007) 1950-1956.

[11]. L. Van der Schueren, K. de Clerck, Halochromic textile materials as innovative ph-sensors, 80 (2012) 47-52.

[12]. T. Guinovart, G. Valdés-Ramírez, J.R. Windmiller, F.J. Andrade, J. Wang, Bandage-based wearable potentiometric sensor for monitoring wound ph, Electroanalysis 26(6) (2014) 1345-1353.

[13]. F. Tang, L. Li, D. Chen, Mesoporous silica nanoparticles: Synthesis, biocompatibility and drug delivery, Adv Mater 24(12) (2012) 1504-34.

[14]. V.-C. Niculescu, Mesoporous silica nanoparticles for bio-applications, Frontiers in Materials 7 (2020).

[15]. A.L. Mohamed, T.A. Khattab, A.G. Hassabo, Color-tunable encapsulated perylene-labeled silica fluorescent hybrid nanoparticles, Results in Chemistry 5 (2023) 100769.

[16]. T.A. Khattab, A.L. Mohamed, A.G. Hassabo, Development of durable superhydrophobic

_____

cotton fabrics coated with silicone/stearic acid using different cross-linkers, Mater. Chem. Phys. 249(122981) (2020).

[17]. I.M. El Nahhal, S.M. Zourab, F.S. Kodeh, F. Babonneau, W. Hegazy, Sol–gel encapsulation of cresol red in presence of surfactants, J. Sol-Gel Sci. Technol. 62(2) (2012) 117-125.

[18]. A.L. Mohamed, T.A. Khattab, M.F. Rehan, A.G. Hassabo, Mesoporous silica encapsulating zns nanoparticles doped cu or mn ions for warning clothes, Results in Chemistry 5 (2023) 100689.

[19]. ASTM Standard Test Method (D3776/D3776M − 09a (Reapproved 2017)), Standard test methods for mass per unit area (weight) of fabric, ASTM International, West Conshohocken, PA, 2018.

[20]. ASTM Standard Test Method (D1777 - 96) (Reapproved 2002), Standard test method for thickness of textile materials, ASTM International, 2017.

[21]. ASTM Standard Test Method (D 4966 - 98), Standard test method for abrasion resistance of textile fabrics (martindale abrasion tester method), ASTM International, 2017.

[22]. ASTM Standard Test Method (D7127 - 13), Standard test method for measurement of surface roughness of abrasive blast cleaned metal surfaces using a portable stylus instrument, ASTM International, West Conshohocken, PA, 2018.

[23]. S.-C. Hsu, T.-M. Don, W.-Y. Chiu, Synthesis of chitosan-modified poly(methyl methacrylate) by emulsion polymerization, J. Appl. Polym. Sci. 86(12) (2002) 3047-3056.

[24]. G.H. Bogush, C.F. Zukoski, Uniform silica particle precipitation : An aggregative growth model, J. Colloid Interface Sci. 142 (1991) 19-34.

[25]. L.P. Singh, S.K. Agarwal, S.K. Bhattacharyya, U. Sharma, S. Ahalawat, Preparation of silica nanoparticles and its beneficial role in cementitious materials, Nanomaterials and Nanotechnology 1 (2011) 9.